Ultrafast vibrational energy transfer at the water-air interface revealed by two-dimensional surface vibrational spectroscopy

Zhen Zhang[1], Lukasz Piatkowski[1], Huib J. Bakker[1] and Mischa Bonn[1,2] *

[1] *FOM-Institute AMOLF, Science Park 104, 1098 XG Amsterdam, The Netherlands*
[2] *Max Planck Institute for Polymer Research, Ackermannweg 10, 55128 Mainz, Germany*

*e-mail: bonn@mpip-mainz.mpg.de

Water is very different from liquids of similar molecular weight and one of its unique properties is the very efficient transfer of vibrational energy between molecules, which is on account of strong dipole-dipole interactions between the O-H oscillators. While we have a sound understanding of such energy transfer in bulk water we know less about how and how quickly transfer occurs at its interface with a hydrophobic phase because of the challenge of specifically addressing the outermost monolayer. Here, we use ultrafast two-dimensional surface-specific vibrational spectroscopy to probe the interfacial energy dynamics of heavy water (D_2O) at the water-air interface. The measurements reveal the presence of surprisingly rapid energy transfer, both between hydrogen-bonded interfacial water molecules (intermolecular), and between O-D groups sticking out from the water surface and those located on the same molecule, pointing towards the water bulk (intramolecular). Vibrational energy transfer occurs on sub-picosecond time scales and its rates and pathways can be quantified directly.

By comparison to other liquids, water has distinct properties reflected in, e.g. its high dielectric constant, anomalous thermal expansion behaviour and high specific heat. These peculiarities can be traced to the unique intermolecular interactions that result from hydrogen bonds between the hydrogen atoms and oxygen atoms of different water molecules. At the surface or interface of water, the water hydrogen-bonded network is abruptly interrupted, giving rise to water molecules with weakened and broken hydrogen bonds. Specifically, at planar

hydrophobic surfaces, including the water-air interface, approximately one in every four interfacial water molecules has a free, non-hydrogen-bonded OH group that protrudes into the hydrophobic phase [1,2].

While structural studies are of obvious importance they do not provide a complete picture of the interface given its highly dynamic, interactive nature. For a complete, molecular-scale understanding of the chemical processes that occur at the water interface one requires insights not only into its structure, but also in the rates and mechanisms of energy transfer and dissipation. In bulk water, energy flow mechanisms and dynamics have been quantified using femtosecond infrared laser techniques [3-5]. The O-H stretch vibrations of the water molecules were found to show rapid resonant (Förster) energy transfer on a time scale <100 fs, largely as a result of the strong dipole-dipole interactions between the O-H oscillators.

The question that presents itself is: how do the local structural changes affect the mechanism and timescale of energy flow at an aqueous interface? The challenge of characterizing the structure of the outermost surface molecules has been met by sum frequency generation (SFG) spectroscopy of their O-H stretch vibrations[1,2,6-12] . In an SFG experiment, infrared and visible laser pulses are overlapped in space and time on the surface, and the sum-frequency of the two laser fields can be generated, but only in the surface region [13]. If the infrared light is resonant with the O-H stretch vibration of surface water, this process is resonantly enhanced. Initial SFG studies, making use of the distinct correlation that exists between the local hydrogen bonding strength and the O-H stretch vibrational frequency of an O-H group in a water molecule, indicated that, in addition to the 'free' O-H groups pointing away from the surface[1,2], different types of hydrogen-bonded interfacial water also exist [1,2,6]. and that the interfacial layer is limited to ~1 monolayer[12].

In bulk water, the O-H vibrations of water molecules were observed to show a very rapid resonant (Förster) energy transfer between water molecules, as demonstrated by measuring the anisotropy dynamics [3] and the ultrafast frequency fluctuations of the O-H stretch vibrations [5]. The frequency fluctuations were measured with two-dimensional infrared (2D-IR) spectroscopy [14,15]. In this technique a vibration is excited with a femtosecond infrared laser pulse and the effect of this excitation on other, nearby vibrations is monitored with a second

femtosecond infrared laser pulse. With this technique, rapid hopping of the excitation over different vibrations was observed. For water at interfaces, a similar efficient vibrational energy transfer was suggested to take place [16 17]. This suggestion was based on time-resolved SFG experiments of the water-fused silica[16] and the water-air[17] interfaces and specifically the absence of any spectral dynamics.

We evaluate interfacial energy flow dynamics, using surface-specific two-dimensional infrared sum-frequency generation (2D-SFG) spectroscopy [18]. This technique, illustrated in Fig. 1, combines the unique capabilities of 2D-IR spectroscopy with the surface specificity and (sub-)monolayer sensitivity of SFG spectroscopy. It enables new insights into energy transfer at water interfaces by investigating the effect of widely tunable (2100-3000 cm^{-1}) excitation pulses of limited spectral width (typically set at 100 cm^{-1}) on the SFG response of interfacial water molecules. As shown below, this scheme allows us to follow the transfer of vibrational energy real-time. We study heavy water (D_2O) rather than normal water, because the intermolecular energy transfer will be slower[19], due to the smaller transition dipole moments of the O-D stretch vibrations, and the narrower homogeneous linewidths compared to the O-H stretch vibrations [19].

Results and discussion

Fig. 2A shows an exemplary 2D-SFG spectrum in the O-D stretch region of the D_2O-air interface at 0 fs delay between excitation and detection pulses. The 2D-SFG spectrum shows the interfacial water response as a function of excitation (horizontal axis) and detection (vertical axis) frequencies (see Methods section and Fig. S1 in the Supplementary Information for details on how the 2D-SFG spectra are recorded and composed). In the experiment, we use a tunable intense pulse of ~100 cm^{-1} bandwidth to resonantly excite the vibrations of specific subsets of D_2O molecules and monitor the effect of the excitation across a wide frequency range using SFG. Along the horizontal (excitation) axis, the linear absorption spectrum of bulk D_2O is shown; the steady state SFG spectrum along the vertical axis reveals the free O-D group, sticking out of the surface, with a vibrational

frequency of 2750 cm^{-1}. Between 2100 and 2600 cm^{-1} a broad-band response of hydrogen-bonded water molecules is apparent.

The excitation causes a temporary reduction of the SFG intensity ('bleach') and the subsequent vibrational relaxation can be followed in real-time through the recovery of the signal. For a completely static, inhomogeneous surface, the response in a 2D spectrum would lie along the diagonal (dashed line; slope=1), because only those water molecules are affected that have been resonantly excited. For a completely homogeneous surface, the response would lie along the horizontal (slope=0), because irrespective of the excitation frequency, the response would always be the same. The observed 2D spectral response in the H-bonded region clearly lies in between these two extremes.

The solid line is a linear fit to the signal maxima at different excitation frequencies, resulting in a line with a slope of 0.23$\pm$0.06. The finite slope of the diagonal response at small delay is direct evidence for the heterogeneity of hydrogen-bonded water molecules at the water-air interface. Water molecules with strong hydrogen bonds absorb at lower frequencies than water molecules with weak hydrogen bonds. The spectral heterogeneity reflecting the distribution of hydrogen bond strengths can be quantified by assuming that the vibrational response can be described by a Gaussian distribution of Lorentzian lines, the latter being characterized by a width Γ_{hom}. Our results reveal that Γ_{hom}= 240 cm^{-1}, with the overall linewidth amounting to 310 cm^{-1}. The large homogeneous linewidth explains the initial spectrally broad response upon excitation with a relatively narrow excitation pulse.

In addition to the response along the diagonal, distinct (off-diagonal) cross peaks are apparent in the 2D spectrum, highlighted by the dotted lines in the 2D spectrum of Fig. 2A. The origin and implications of these cross peaks for the interfacial heterogeneity will be discussed in more detail below.

The spectral heterogeneity within the H-bonded region reflecting the structural inhomogeneity is very short-lived. Fig. 2B shows transient spectra at different delay times, following excitation using a pump pulse centered at a relatively high frequency of 2625 cm^{-1}. The maximum in the signal shifts from high to low frequencies, i.e.

the signal displays spectral diffusion on a ~600 fs timescale. Vibrational relaxation of the O-D stretch mode occurs with a time constant of 1.0±0.1 ps (see Supporting Online Material, section 'Determination of vibrational lifetime'; Fig. S2). For long delay times, the signal is dominated by thermal effects, which give rise to both positive and negative signals due to a blueshift of the SFG response. The time constant for the thermal relaxation step was not directly quantified, but, as evident from Figs. 3D and 3E, the thermal signal apparent at 6000 fs delay (characterized also by an induced SFG signal around ~2630 cm^{-1} due to a blueshift of the SFG response at elevated temperatures) exhibits a delayed ingrowth[20], and at 2100 fs the thermal signal is still weak in comparison to the signal of the excited OD vibrations. In our analysis, we can therefore neglect contributions from the thermal signal to spectral diffusion for timescales up to ~3 ps.

The spectral diffusion can be quantified from the time-dependent slope of the diagonal response of the 2D spectra, as shown in Fig. 3F. Such spectral diffusion may be due to structural relaxation at the water interface, so that by H-bond rearrangement, strongly H-bonded water molecules can become weakly bonded and vice versa. However, spectral diffusion is also indicative of intermolecular energy transfer: For bulk H_2O, very efficient transfer of vibrational energy between different water molecules has been demonstrated [3,5,19,21]. This energy transfer is caused by dipole-dipole coupling between different O-D groups and is expected to contribute significantly to the spectral diffusion within the O-D stretch vibrational band, as vibrational energy transfer can occur between differently hydrogen-bonded O-D groups, with different frequencies. While we cannot exclude a contribution to the dynamics from structural relaxation, we first explore whether vibrational energy transfer, expected to be very efficient also at the interface, provides a sufficient explanation of the observed spectral dynamics.

Efficient interfacial intermolecular energy transfer

We model the decay of the time-dependent slope $S(t)$, which is a measure of heterogeneity**,** using the model for resonant energy transfer in D_2O [19]. The decay of the slope is directly proportional to the decay of the frequency-frequency correlation function, as demonstrated previously for conventional 2D-IR[22]. The decay of

this correlation function originates from energy transfer between OD groups of different frequency. Assuming that energy transfer is the only mechanism scrambling the frequency, and that each transfer step leads to a complete randomization of the vibrational frequency, we can express the slope at time t for a concentration of O-D groups c_{OD}[in M/Å^3]=2×c_{D2O} as (see supplementary information, section 'Model for interfacial, intermolecular energy transfer' for details):

$$S(t) = S_0 \, exp\left(-(4\pi^{3/2}/3) c_{OD} N_A \sqrt{r_0^6 t / T_1}\right), \qquad (1)$$

where N_A is Avogadro's number, r_0 is the distance over which the energy transfer occurs with 50% efficiency, and S_0 is the initial slope value. The dipole-dipole coupling strength is represented by the term $\sqrt{r_0^6/T_1}$. This term is proportional to the transition dipole moments of donor and acceptor. The Förster radius r_0 is the distance between donor and acceptor for which energy transfer plays a role within the lifetime T_1. Hence, if T_1 increases, r_0 also increases, not because there is a change in the dipole-coupling, but because there is more time for the energy transfer to take place within the lifetime of the excitation. Following Refs. [3,19], the radius r_0 is referenced here to T_1=1700 fs, the intrinsic vibrational lifetime of the isolated O-D stretch vibration in bulk H_2O. We note that T_1 is much shorter than the radiative lifetime of the transition, and that thermal relaxation effects are ignored in the analysis.

Using this equation we find a very good description of the dynamics with r_0 = 1.9±0.2 Å. This value is appreciably smaller than the value of r_0 = 2.3±0.2 Å found for bulk D_2O [19]. This indicates that energy transfer between the O-D vibrations is slower at the D_2O surface than in the bulk. This slower energy transfer can likely be attributed to the lower density of acceptors for D_2O molecules near the interface. For the top-most layer of D_2O molecules, the number density of available acceptors is expected to be only half the number density of D_2O molecules in the bulk. In the supplementary information (section 'Model for interfacial, intermolecular energy transfer'), we derive a modified equation for the energy exchange between an O-D group at the surface and a bulk-like hemisphere below it:

$$S(t) = S_0 \, exp\left(-(2\pi^{3/2}/3) c_{OD} N_A \sqrt{r_0^6 t / T_1}\right) \qquad (2)$$

This equation differs from the previous equation in the two times smaller exponential factor. The result of fitting this model to the data is shown as the line in Fig. 3F. Fitting this model we find r_0 = 2.4±0.3 Å, indistinguishable from the 2.3 Å found for bulk D_2O [19]. The success of equation (2) in describing the data implies that the 2D-IR SFG technique probes the D_2O-air interface over a penetration depth less than r_0. As r_0 is similar to the intermolecular separation in liquid D_2O, this finding demonstrates that the 2D-SFG technique only probes the outermost molecules of the D_2O surface.

While this energy transfer model provides a quantitative description of the observed spectral dynamics, this does not prove the model is correct. A rigorous test of the validity of the model is a measurement of the spectral diffusion rate in dependence of the isotope dilution[3,19]. In the Supporting Online Material (section 'Isotopic dilution leads to slow-down of the intermolecular energy transfer'; Fig. S3), we present results for isotopically diluted water, which reveal, for a 2-fold diluted sample, a slow-down of the spectral diffusion dynamics by a factor of 2. These results can be quantitatively reproduced by the model.

The observation that the energy transfer model provides a quantitative, complete and sufficient description of the observed spectral dynamics, suggests that the homogeneous linewidth inferred from the data at time zero contains little contribution from spectral diffusion and that structural dynamics do not contribute significantly to the spectral diffusion process. The latter observation is not very surprising, considering the very short timescale on which the spectral diffusion due to Förster energy transfer occurs. 2D-IR studies of the structural dynamics of isotopically diluted water samples, for which there is no resonant energy transfer, showed the presence of only a minor structural relaxation component on a 100 fs time scale [23,24]. The dominant structural rearrangement of the hydrogen bond network of bulk water was observed to take place on longer timescales.

The 2D-SFG spectra thus allow us to follow the dynamics of intermolecular energy transfer between interfacial water molecules in real-time, revealing the predominance of dipole-dipole interactions in conjunction with the

simple truncation of the water structure at the interface. The 2D-SFG spectroscopy results presented here allow for the quantification of the energy flow rate. The fact that simple geometric arguments (energy transfer into a half-sphere) completely account for the timescale on which resonant energy transfer occurs at the water-air interface, is consistent with the molecularly sharp density profile at the interface [25,26].

Efficient interfacial intramolecular energy transfer

We now turn to the off-diagonal cross peaks observed in the 2D spectra at (excitation, detection) frequencies (in cm^{-1}) of both (2580, 2750) and (2750, 2580), highlighted as dotted circles in Fig. 2A. The presence of these cross peaks implies strong coupling resulting in energy transfer between the free O-D stretch and a vibration on the blue side of the hydrogen-bonded peak. Considering the large energy mismatch between these two frequencies, this coupling cannot be due to resonant dipole-dipole interactions between the two OD groups, since significant energy matching is required. The interaction must therefore rely on an interaction between the donor and acceptor vibration in which the energy mismatch is taken away or supplied by a third, low-frequency degree of freedom. Hence, the coupling is at least of third-order in the vibrational coordinates, i.e. of the donor, the acceptor, and the low-frequency mode, which means that this coupling is anharmonic. The anharmonic coupling is most likely through-bond and therefore of *intra*- rather than of *inter*-molecular nature. This means that the resonance at 2580 cm^{-1} on the blue side of the H-bonded peak belongs to the O-D group that is part of the same water molecule that has a free O-D group at 2750 cm^{-1} sticking out of the surface. This assignment agrees with previous polarization-resolved [27] and isotope-dependent [12] static SFG experiments, which indicated that the H-bonded O-D group attached to the free O-D has a vibrational frequency on the very blue side of the broad hydrogen-bonded absorption band. The 2D-spectra presented here reveal unambiguously the strong coupling between these two O-D groups.

We investigate the dynamics of the (2750, 2750) and (2750, 2580) spectral features, as shown in Figure 4. The dynamics of the cross peak reveals that the mechanism of vibrational relaxation is rather intricate: the somewhat delayed in-growth of the cross peak indicates rapid vibrational energy transfer from the free O-D to

the H-bonded O-D within the same D_2O molecule. The rapid equilibration of vibrational energy between the two modes is followed by a decay due to vibrational relaxation, presumably through the H-bonded O-D group. A model that includes in parallel both the energy equilibration and the vibrational relaxation provides a very good description of the data, as shown by the solid lines in Fig. 4 (see Supplementary Information, section 'Rate equation model for interfacial, intramolecular energy transfer'). We obtain a time constant of k_1=300±60 fs for the energy transfer from the free O-D to the hydrogen-bonded O-D. The time constant for the reverse process fulfills detailed balance $k_1 / k_{-1} = exp\left(-(2750-2580)/k_B T\right)$ and equals k_{-1}=780±150 fs. Vibrational relaxation of the H-bonded O-D group occurs with a time constant of 900±50 fs – in good agreement with the direct measurement of the ~1 ps lifetime inferred from the diagonal response, exciting and detecting the H-bonded OD groups. This lifetime is similar to the previously reported ~1 ps lifetime of the free O-H of H_2O[16]. For this free O-H the relaxation is expected to take a similar path as the free O-D at the D_2O surface, namely a rapid equilibration of the vibrational energy over the two O-H groups of the H_2O molecule, followed by the cooperative relaxation of the two groups. Here we can resolve the first equilibration process thanks to the dynamics of the cross-peaks in the 2D-SFG spectra. Thereby we find that the free OD groups serve as efficient antennas for vibrational energy, and rapidly transfer this energy to the H-bonded OD group within the same molecule because of efficient intramolecular anharmonic coupling. Resonant dipole-dipole coupling of the H-bonded OD group with other water molecules will then delocalize the vibrational energy further.

In summary, we demonstrate that 2D-IR SFG data reveal the occurrence of surprisingly fast intra- and intermolecular energy transfer processes at aqueous interfaces. The results show that energy transfer among OD stretching modes of water on the surface is rapid and efficient and that OD excitations move both along the surface plane and down into the bulk. This result highlights the uniqueness of water because no other known substance has such fast and efficient intermolecular vibrational energy transfer. This information on interfacial aqueous energy flow patterns contribute to our understanding of chemistry at aqueous interfaces, as chemical reactions at aqueous surfaces, be it on catalytic water interfaces, atmospheric chemistry or at cell membrane surfaces.

Methods

The energy transfer and the structure of water have been studied using femtosecond SFG-2D-IR spectroscopy. SFG intrinsically has monolayer sensitivity and surface specificity. [13] The SFG-2D-IR method has been introduced recently [18,28]. In our SFG-2D-IR experiment, we use an IR-pump-SFG probe scheme, where the pump spectrum is spectrally narrow and continuously tuned across the absorption band.

For the detection process, broadband mid-IR and narrowband visible upconversion pulses are mixed at the interface to generate a conventional SFG signal. These pulses are generated by frequency conversion processes that are pumped with the near-infrared 800 nm pulses derived from a high energy Ti:Sapphire amplifier system. This system is a regenerative amplifier ("Legend Duo", Coherent) that delivers 40 fs pulses with a pulse energy of 6 mJ per pulse at a repetition rate of 1 kHz. We use about 4.5 mJ to pump an optical parametric amplifier (HE-TOPAS, Light Conversion). The produced signal and idler pulses are used in a difference frequency mixing process in a silver gallium disulphide ($AgGaS_2$) crystal resulting in 80 µJ pulses, tunable around a central wavelength of ~4000 nm (~2500 cm^{-1}), a pulse duration of ~60 fs full width at half maximum (FWHM), and a spectral bandwidth of ~400 cm^{-1} FWHM. These pulses spectrally cover the whole vibrational band of water and we use them in the SFG probing process. The remaining 1.5 mJ of 800 nm pulses travel through an etalon (SLS) resulting in narrowband pulses (15 cm^{-1} FWHM) used in the SFG process. The overall spectral resolution is primarily limited by the bandwidth of these pulses, and thus amounts to 15 cm^{-1}.

For the SFG-2D-IR experiment, an additional high intensity and narrow-band pump pulse is required to excite ground state molecules to the v=1 vibrational state. This high-intensity infrared pump pulse is generated in an independent parametric conversion process. We use the residual 800 nm and idler pulses from the TOPAS. The idler pulses are further doubled in a BBO crystal, resulting in pulses with a central wavelength of ~1000 nm. The doubled idler and 800 nm pulses are then used for a difference frequency mixing process in a $LiNbO_3$ crystal. This process results in ~45 µJ pump pulses, with a central wavelength ranging between 2100 – 2900 cm^{-1} and a pulse duration less than 200 fs. Combined with the 60 fs probe pulse, the time resolution, determined by the

cross correlation between pump and probe, in the experiments is approximately 200 fs. The bandwidth of the pump pulses varies between 80 – 150 cm^{-1}. Both pump and probe pulses are continuously monitored with a frequency resolved IR detection setup consisting of an ORIEL monochromator and a 2x32 pixel, mercury-cadmium-telluride (MCT) array detector. Different pump frequencies (2275, 2350, 2425, 2500, 2575, 2625, 2750 and 2825 cm^{-1}) have been used to excite the hydrogen bond and the free OD bond. The spectra of these pulses are shown in Supplementary Information figure S1. All experiments have been performed at least twice to ensure their reproducibility.

2D-SFG spectra were composed from the transient spectra recorded at delay times of -1200, -600, -300, 0, 300, 600, 900, 1200, 2100, 3000 and 6000 fs following standard procedures [29]: vertical cuts at specific excitation frequencies were calculated using a weighted average of transient spectra at different pump frequencies, with weights determined by the relative intensities of the pump spectra at that frequency, as inferred from the spectra in Fig. S1. The resulting 2D-SFG spectrum was Fourier filtered to remove high-frequency noise from the detection, where care was taken to retain the 15 cm^{-1} experimental resolution, i.e. to avoid smearing out experimental features in the recorded 2D spectrum. Within the frequency window 2400-2800 cm^{-1}, the 2D spectra could be determined with an accuracy better than 1% of the original SFG spectra; outside this window the low probe energy causes some noise.

In the experiment, the pump frequency which determines the horizontal axis of the 2D vibrational spectrum., is scanned. The vertical axis is determined by the infrared frequency of the SFG probing process. The IR pump, IR probe and VIS pulses with energies of 12, 6.5 and 10 μJ/pulse, respectively, are propagated in a vertical plane and have respective incident angles of 56°/40°/70° with respect to the surface normal. The polarization of the SFG/VIS/IR beam was controlled using a λ/2 plate and were S/S/P in all experiment; the polarization of the pump pulses was P. The third-order cross correlation between the IR pump, IR probe and visible pulses generated from the heavy water surface was used to optimize the spatial overlap and to define the position of τ=0.

D_2O (Cambridge Isotope Laboratories. Inc., 99.96 atom %D) was used without further purification (pH=~5.5). The Teflon sample trough was cleaned with piranha solution (3:1 volume ratio of sulfuric acid and 30% hydrogen peroxide solution) and rotated in order to avoid accumulated heating by the laser pulses. The vertical sample position was controlled by a feedback loop to compensate for water evaporation. The whole setup was enclosed and flushed with N_2 gas in order to remove spectral distortions originating from CO_2 absorption in the air.

Supporting Online Material: Determination of the vibrational lifetime of the H-bonded OD groups ; Derivation of the intermolecular energy transfer rates; Model to describe interfacial intramolecular energy transfer; Results and discussion of isotopic dilution experiments; Figs. S1, S2 and S3; References.

Correspondence and requests for materials should be addressed to MB.

Author contributions: MB and HJB designed the research project: ZZ and LP performed the experiments: MB, ZZ and LP analyzed the data: MB wrote the manuscript: All authors discussed the results, designed experiments and commented on the manuscript.

Acknowledgements: We are grateful to Jan Versluis and Marc Jan van Zadel for their expert help and support and to Iliya Cerjak for the graphics.

Figure captions:

Figure 1: Experimental scheme for 2-dimensional SFG spectroscopy: A tunable infrared pulse excites a subset of water molecules from the ground (v=0) to the first vibrationally excited (v=1) state. The interfacial response is detected over a wide frequency range as a function of delay, using a pair of infrared and visible detection pulses (a) that generate light at their sum frequency at the interface (b, c).

Figure 2: 2-dimensional SFG spectroscopy of the D_2O water-air interface. (a) 2D spectrum recorded at zero delay time between excitation and detection pulses, along with the linear absorption (horizontal) and SFG (vertical) spectra of D_2O. The 2D spectrum is reconstituted from difference spectra between excited and unexcited SFG spectra, at various excitation frequencies. Red (blue) indicates a decrease (increase) in the SFG signal, as shown by the scale bar next to panel (b). The dashed line indicates the diagonal, with a slope of 1; the solid line indicates the average slope (0.23) of the main, broad response. A second diagonal peak appears at the free O-D at 2750 cm^{-1}; off-diagonal intensity (dotted ovals; cross peaks) appears at (2580, 2750) and (2750, 2580). (b) Direct observation of spectral diffusion at the water-air interface. Frequency-resolved transient SFG spectra at different delay times after excitation at 2625 cm^{-1} reveal a red shift of the maximum signal. The dashed line is a guide to the eye. The intensity increase above 2600 cm^{-1} observed at delays > 3 ps is due to the ingrowth of thermal effects following vibrational relaxation.

Figure 3: 2-dimensional SFG spectra of the D_2O water-air interface at various delay times after the excitation (a-e). The solid lines represent the IR frequency corresponding to the maximum SFG response as a function of the excitation frequency. Red (blue) indicates a decrease (increase) in the SFG signal, as shown by the scale bar next to panel (e), which is valid for panels (a)-(e).The slopes of the solid lines are plotted as a function of delay in panel f. The solid line in panel f is the result of a model calculation that accounts for the spectral diffusion by resonant Förster energy transfer (see main text) with r_0 = 2.4±0.3 Å (error indicated by the grey area).

Figure 4: Ultrafast intramolecular energy transfer within interfacial water molecules. Dynamics of the resonance of the free O-D vibration excited and detected at 2750 cm^{-1}, and the cross peak excited at 2750 cm^{-1} and detected at 2580 cm^{-1}. (a) The signal of the free O-D stretch at 2750 cm^{-1} shows a rapid initial decay while the cross-peak shows a delayed rise. These dynamics are due to energy transfer from the excited free O-D vibration sticking out of the surface to the O-D group that is located on the same water molecule and pointing into the bulk. After equilibration, the two modes relax together with the same effective rate. (B) The cartoon on the right depicts the interfacial energy flow processes with the time constants obtained from the experiments.

References

1 Du, Q., Superfine, R., Freysz, E. & Shen, Y. R. Vibrational spectroscopy of water at the vapor water interface. *Phys. Rev. Lett.* **70**, 2313-2316 doi: 10.1103/PhysRevLett.70.2313 (1993).

2 Du, Q., Freysz, E. & Shen, Y. R. Surface vibrational spectroscopic studies of hydrogen-bonding and hydrophobicity. *Science* **264**, 826-828 doi: 10.1126/science.264.5160.826 (1994).

3 Woutersen, S. & Bakker, H. J. Resonant intermolecular transfer of vibrational energy in liquid water. *Nature* **402**, 507-509 doi: 10.1038/990058 (1999).

4 Lock, A. J., Woutersen, S. & Bakker, H. J. Ultrafast energy equilibration in hydrogen-bonded liquids. *J. Phys. Chem. A* **105**, 1238-1243, doi:10.1021/jp003158e (2001).

5 Cowan, M. *et al.* Ultrafast memory loss and energy redistribution in the hydrogen bond network of liquid H_2O. *Nature* **434**, 199-202, doi:10.1038/nature03383 (2005).

6 Scatena, L., Brown, M. & Richmond, G. Water at hydrophobic surfaces: Weak hydrogen bonding and strong orientation effects. *Science* **292**, 908-912 doi: 10.1126/science.1059514 (2001).

7 Shen, Y. R. & Ostroverkhov, V. Sum-frequency vibrational spectroscopy on water interfaces: Polar orientation of water molecules at interfaces. *Chem. Rev. (Washington, DC, U. S.)* **106**, 1140-1154, doi:10.1021/cr040377d (2006).

8 Gopalakrishnan, S., Liu, D. F., Allen, H. C., Kuo, M. & Shultz, M. J. Vibrational spectroscopic studies of aqueous interfaces: Salts, acids, bases, and nanodrops. *Chem. Rev. (Washington, DC, U. S.)* **106**, 1155-1175, doi:10.1021/cr040361n (2006).

9 Sovago, M., Campen, R. K., Bakker, H. J. & Bonn, M. Hydrogen bonding strength of interfacial water determined with surface sum-frequency generation. *Chem. Phys. Lett.* **470**, 7-12, doi:10.1016/j.cplett.2009.01.009 (2009).

10 Tian, C. S. & Shen, Y. R. Sum-frequency vibrational spectroscopic studies of water/vapor interfaces. *Chem. Phys. Lett.* **470**, 1-6, doi:10.1016/j.cplett.2009.01.016 (2009).

11 Nihonyanagi, S., Yamaguchi, S. & Tahara, T. Water Hydrogen Bond Structure near Highly Charged Interfaces Is Not Like Ice. *J. Am. Chem. Soc.* **132**, 6867-+, doi:10.1021/ja910914g (2010).

12 Stiopkin, I. V. *et al.* Hydrogen bonding at the water surface revealed by isotopic dilution spectroscopy. *Nature* **474**, 192-195, doi:10.1038/nature10173 (2011).

13 Shen, Y. R. Surface-Properties Probed by 2^{nd} Harmonic and Sum-Frequency Generation. *Nature* **337**, 519-525 doi:10.1038/337519a0 (1989).

14 Cho, M. H. Coherent two-dimensional optical spectroscopy. *Chem. Rev. (Washington, DC, U. S.)* **108**, 1331-1418, doi:10.1021/cr078377b (2008).

15 Khalil, M., Demirdoven, N. & Tokmakoff, A. Coherent 2D IR spectroscopy: Molecular structure and dynamics in solution. *J. Phys. Chem. A* **107**, 5258-5279, doi:10.1021/jp0219247 (2003).

16 McGuire, J. A. & Shen, Y. R. Ultrafast vibrational dynamics at water interfaces. *Science* **313**, 1945-1948, doi:10.1126/science.1131536 (2006).

17 Smits, M., Ghosh, A., Sterrer, M., Müller, M. & Bonn, M. Ultrafast Vibrational Energy Transfer between Surface and Bulk Water at the Air-Water Interface. *Phys. Rev. Lett.* **98**, 098302, doi:10.1103/PhysRevLett.98.098302 (2007).

18 Bredenbeck, J., Ghosh, A., Nienhuys, H. K. & Bonn, M. Interface-Specific Ultrafast Two-Dimensional Vibrational Spectroscopy. *Acc. Chem. Res.* **42**, 1332-1342, doi:10.1021/ar900016c (2009).

19 Piatkowski, L., Eisenthal, K. B. & Bakker, H. J. Ultrafast intermolecular energy transfer in heavy water. *Phys. Chem. Chem. Phys.* **11**, 9033-9038, doi:10.1039/b908975f (2009).

20 Lock, A. J. & Bakker, H. J. Temperature dependence of vibrational relaxation in liquid H2O. *J. Chem. Phys.* **117**, 1708-1713, doi:10.1063/1.1485966 (2002).

21 Kraemer, D. *et al.* Temperature dependence of the two-dimensional infrared spectrum of liquid H2O. *Proc. Natl. Acad. Sci. U. S. A.* **105**, 437-442, doi:10.1073/pnas.0705792105 (2008).
22 Kwak, K., Park, S., Finkelstein, I. J. & Fayer, M. D. Frequency-frequency correlation functions and apodization in two-dimensional infrared vibrational echo spectroscopy: A new approach. *J. Chem. Phys.* **127**, 124503 doi:10.1063/1.2772269 (2007).
23 Asbury, J. B. *et al.* Dynamics of water probed with vibrational echo correlation spectroscopy. *J. Chem. Phys.* **121**, 12431-12446, doi:10.1063/1.1818107 (2004).
24 Loparo, J. J., Roberts, S. T. & Tokmakoff, A. Multidimensional infrared spectroscopy of water. I. Vibrational dynamics in two-dimensional IR line shapes. *J. Chem. Phys.* **125**, 194521, doi:10.1063/1.2382895 (2006).
25 Taylor, R. S., Dang, L. X. & Garrett, B. C. Molecular dynamics simulations of the liquid/vapor interface of SPC/E water. *J. Phys. Chem.* **100**, 11720-11725 doi:10.1021/jp960615b (1996).
26 Mucha, M. *et al.* Unified molecular picture of the surfaces of aqueous acid, base, and salt solutions. *J. Phys. Chem. B* **109**, 7617-7623, doi:10.1021/jp0445730 (2005).
27 Gan, W., Wu, D., Zhang, Z., Feng, R. & Wang, H. Polarization and experimental configuration analyses of sum frequency generation vibrational spectra, structure, and orientational motion of the air/water interface. *J. Chem. Phys.* **124**, 114705 doi: 10.1063/1.2179794 (2006).
28 Bredenbeck, J., Ghosh, A., Smits, M. & Bonn, M. Ultrafast two dimensional-infrared spectroscopy of a molecular monolayer. *J. Am. Chem. Soc.* **130**, 2152-+, doi:10.1021/ja710099c (2008).
29 Cervetto, V., Helbing, J., Bredenbeck, J. & Hamm, P. Double-resonance versus pulsed Fourier transform two-dimensional infrared spectroscopy: An experimental and theoretical comparison. *J. Chem. Phys.* **121**, 5935-5942, doi:10.1063/1.1778163 (2004).

Supporting Online Material for Manuscript:

"Ultrafast vibrational energy transfer at the water-air interface revealed by two-dimensional surface vibrational spectroscopy"

Zhen Zhang, Lukasz Piatkowski, Huib J. Bakker and Mischa Bonn

Methods

Different pump frequencies (2275, 2350, 2425, 2500, 2575, 2625, 2750 and 2825 cm^{-1}) have been used to excite the hydrogen bond and the free OD bond. The spectra of these pulses are shown in figure S1.

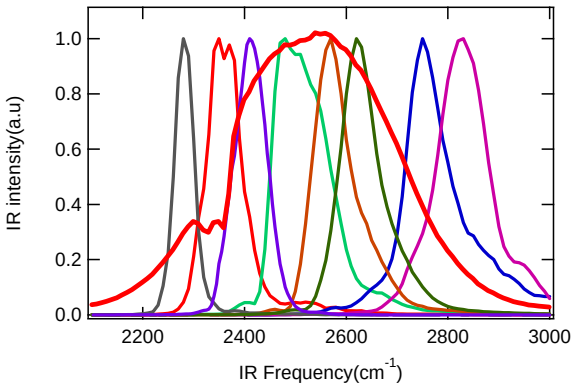

Fig. S1: Pump (narrow) and probe (broad) spectra used in recording the 2D spectra reported in the main manuscript.

Determination of vibrational lifetime

Exciting and detecting the differential SFG signal near the peak of the SFG spectrum, provides us with a relatively good way of determining the lifetime of the O-D stretch vibration, as the effects of spectral diffusion and slow ingrowth of the thermal signal are minimized. At the peak of the response, the derivative of the spectral response is zero, and the vibrational lifetime shows a minimal sensitivity to spectral changes.

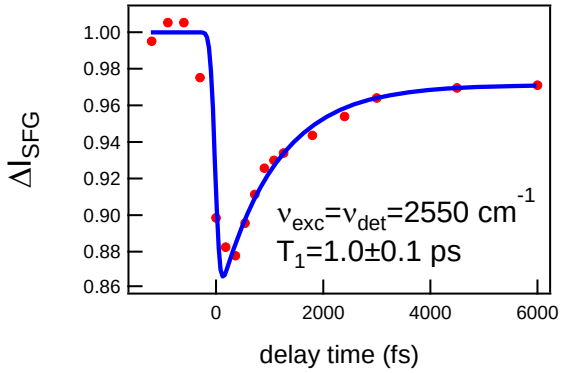

Fig. S2: Differential SFG signal with excitation and detection spectra tuned to 2550 cm^{-1}. A single-exponential fit to the data reveals a lifetime of 1 ps.

Model for interfacial, intermolecular energy transfer

Here, we derive the formula describing vibrational energy transfer due to dipole-dipole coupling based on Förster's original derivation of the formula describing dipole-dipole coupling between dye molecules [1] and later work, where the Förster's formulation has been used to describe dipole-dipole coupling in neat water [2,3].

When a molecule at $t = 0$ is excited, the probability that this molecule is still excited at $t = \tau$ is equal to:

$$\rho(\tau) = \sum_{j=1}^{N_{OD}} \exp(-k_j \tau),$$

where N_{OD} (N_{OD}=2N$_{D2O}$) is the number of accepting oscillators and k_j is the rate constant for the vibrational energy transfer. If we assume that the resonant transfer rate is independent of the relative orientations between donor and acceptor molecules, and results from dipole-dipole couplings, the energy transfer rate k_j depends as follows on the relative distance between accepting and donating molecule r_j:

$$k_j = \frac{1}{T_1}\left(\frac{r_0}{r_j}\right)^6,$$

Here T_1 is the vibrational lifetime in the absence of the energy transfer and r_0 is the so-called Förster radius, which defines the distance at which the rates of vibrational relaxation and resonant vibrational energy transfer are equal (i.e. the distance for which there is a probability of 50% that energy transfer occurs within the lifetime).

The acceptor molecules are distributed randomly over the sample, which for the top most layer at the surface has a hemispherical geometry. The probability to find an accepting molecule at a distance r_j and r_j+dr_j is equal to the surface area of the hemisphere normalized to the total volume of the sample V:

$\eta(r) = \frac{2\pi r_j^2 dr_j}{V}$, where $V = \frac{2\pi R^3}{3}$ and R is a radius of the hemisphere.

Combining the two probabilities: the probability that the molecule is excited at $t=\tau$ and the probability of finding an accepting molecule for each of the N_{OD} oscillators in the system, we arrive at:

$$\rho(\tau) = \left\{\frac{2\pi}{V}\int_0^R \exp\left[-\frac{\tau}{T_1}\left(\frac{r_0}{r}\right)^6\right] r^2 dr\right\}^{N_{OD}}.$$

Performing the integration we obtain:

$$\rho(\tau) = \left\{\exp\left[-\frac{\tau}{T_1}\left(\frac{r_0}{R}\right)^6\right] - \sqrt{\frac{\pi\tau}{T_1}\left(\frac{r_0}{R}\right)^6} + \sqrt{\frac{\pi\tau}{T_1}\left(\frac{r_0}{R}\right)^6}\, Erf\left[\sqrt{\frac{\pi\tau}{T_1}\left(\frac{r_0}{R}\right)^6}\right]\right\}^{N_{OD}}.$$

We can express the concentration of the sample as a number of molecules in the volume $C_{OD} = \frac{3N_{OD}}{2\pi R^3 N_A}$ [mol/Å^3] where N_A is Avogadro's number. Using this expression we can eliminate the hemisphere radius from the above equation. Performing the power expansion in terms of $1/N_{OD}$ we arrive at:

$$\rho(\tau) = \left\{1 - \frac{2\pi^{3/2} C_{OD} N_A}{3} \sqrt{\frac{r_0^6 \tau}{T_1}} \left(\frac{1}{N_{OD}}\right) + \alpha \left(\frac{1}{N_{OD}}\right)^2\right\}^{N_{OD}}$$

For bulk water (or, equivalently, for a hemisphere of water), the number of accepting molecules $N \to \infty$ so the nonlinear terms $(1/N_{OD})^m$ become small and we neglect them. Doing so we obtain the well-known expression:

$$\rho(\tau) = \exp\left(\frac{2}{3}\pi^{3/2} C_{OD} N_A \sqrt{r_0^6 \tau / T_1}\right).$$

Using that the decay of the slope of the heterogeneous response is proportional to the probability of the excited molecule to transfer its vibrational energy $S(\tau) \propto \rho(\tau)$, we arrive with the final expression:

$$S(\tau) \propto \exp\left(-(2\pi^{3/2}/3) C_{OD} N_A \sqrt{r_0^6 \tau / T_1}\right)$$

The above expression describes resonant vibrational energy transfer for a molecule located at the surface, and assumes that an energy transfer step leads to complete randomization of the vibrational frequency, i.e. that an energy transfer step leads to a complete decay of the frequency-frequency correlation function for a given OD group. This means that the ensemble-averaged correlation function decays with the time-dependent energy transfer probability (i.e. $S(\tau) \propto \rho(\tau)$). This model does not include thermal effects that grow in at later times. Note that the rate of energy transfer is two times smaller than the rate of energy transfer of a molecule located in the bulk. This difference arises from the integration over acceptors in a hemisphere, rather than over acceptors in a sphere.

Isotopic dilution leads to slow-down of the intermolecular energy transfer

The intermolecular energy transfer model quantitatively reproduces the time-dependent slope of the 2D-SFG spectra reported here (Fig. 3F in main text). While this energy transfer model provides a complete and sufficient description of the observed spectral dynamics, this does not prove the model is correct. A stringent test of the validity of the model is a measurement of the spectral diffusion rate in dependence of isotope dilution (as some of us have done before for bulk water[2,4]). The result of spectral diffusion measurements on a 1:1 mixture of D_2O and H_2O is shown in Fig. S3. The figure shows frequency-resolved transient SFG spectra at different delay times after excitation at 2625 cm-1 for pure D_2O (upper left), and at 2560 cm^{-1} for a 1:1 H2O/D2O mixture (upper right). The left panel is identical to Fig. 2B in the main text. The conventional SFG spectrum changes slightly upon isotopic dilution[5], and therefore somewhat different excitation frequencies were chosen to achieve the same excitation density. It is evident from these results that the spectral diffusion dynamics slows down upon isotopic dilution. The results are summarized in the lower panel, which shows the frequency of the bleach maximum at different delay times. The solid lines in the lower panel are calculations following the intermolecular energy transfer model presented above, and are the same as those in the two upper panels. These results are in quantitative agreement with the Förster energy transfer model, showing the expected slow-down of the spectral diffusion dynamics. Given that the structural, molecular dynamics remain unchanged upon isotopic dilution, this proves that the spectral diffusion, and time-dependent slopes of the 2D spectra, are the result of efficient intermolecular energy transfer, and justifies the use of the proposed model. The model can be used to describe both the time-dependence of the slope of the 2D spectra and the temporal evolution of the bleach (fig. S3), as both observables decay as a result of the same process of intermolecular vibrational energy transfer, which causes a decay of the frequency-frequency correlation function. The slope of the main feature in the 2D spectrum, however, reflects the response of all water molecules; the response at one bleach frequency reflects only those water molecules that have been excited. We note that the energy transfer shows an $exp(-C_{OD}\sqrt{t})$ dependence, as borne out by the experiments. The $\sqrt{t}$ -dependence results from the statistical distribution of intermolecular distances. The difference between high and low concentration is primarily the larger fraction of short intermolecular distances at high concentrations that leads to a stronger contribution of fast decays to the signal. These fast decays at high concentrations dominate the signal at early delay times. At later times, the contribution of fast intermolecular energy transfer has vanished, and for all concentrations the signal decay is determined by donating and accepting dipoles at large intermolecular separations. It is thus a characteristic property of resonant energy transfer that the decays at different concentrations will become increasingly similar with increasing time delay. The difference lies in the early times.

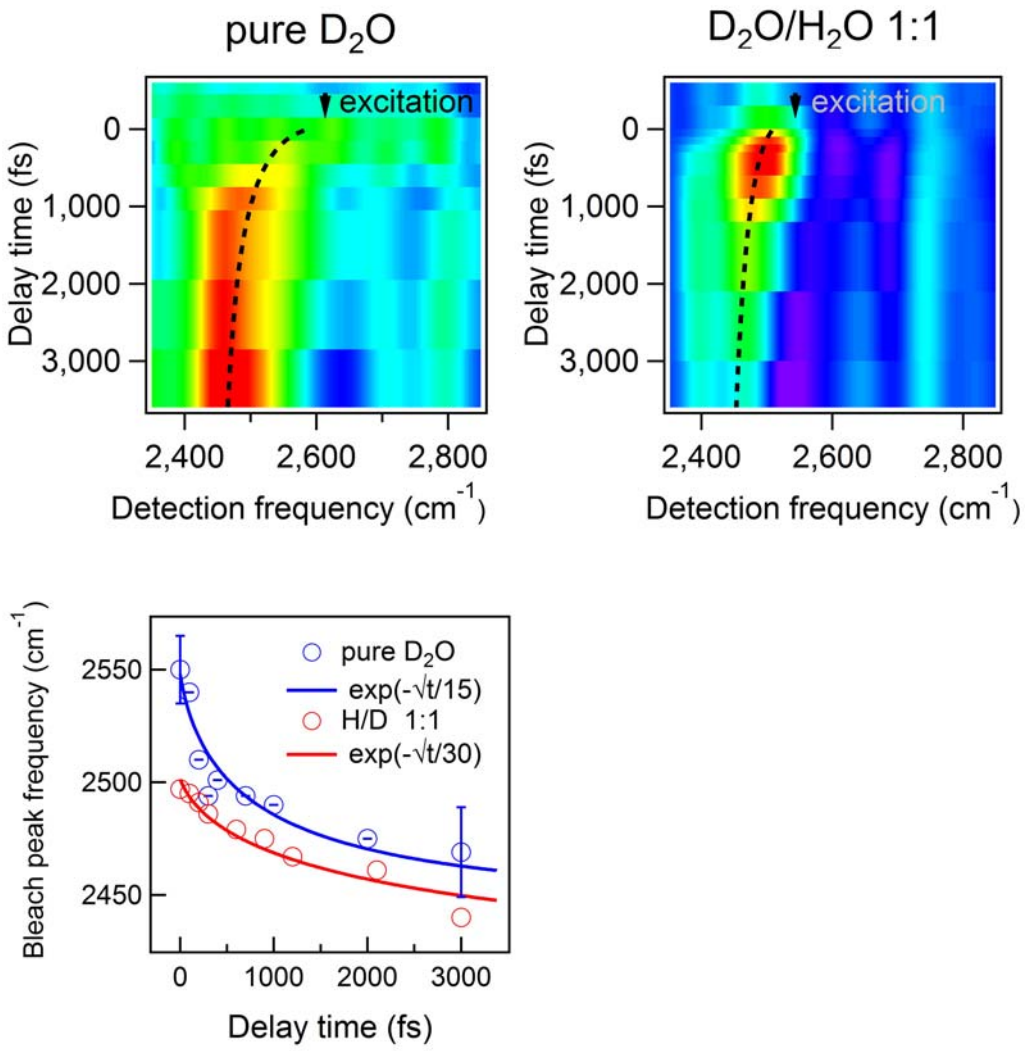

Fig. S3: Isotopic dilution measurements show that spectral diffusion slows down in proportion to isotope content. Frequency-resolved transient SFG spectra at different delay times after excitation at 2625 cm^{-1} for pure D_2O (upper left) and 2560 cm^{-1} for a 1:1 H_2O/D_2O mixture (upper right). Both experiments reveal a red shift of the maximum signal. The upper left panel is identical to Fig. 2B in the main text. The dashed lines are calculations following the intermolecular energy transfer model. The experiments for a 1:1 H/D isotopically diluted sample reveals a 2-fold slowdown of the spectral diffusion dynamics, precisely as expected for energy transfer, due to the 2-fold lowering of the concentration of OD groups C_{OD}. The results are summarized in the lower panel, which shows the frequency of the bleach maximum at different delay times. The lines correspond to those in the two upper panels, and quantitatively confirm the expected slow-down by a factor of 2 for the 2-fold diluted sample.

Rate equation model for interfacial, intramolecular energy transfer

In the following, we will present the model and the corresponding differential equations describing the intramolecular coupling process between the free OD groups (denoted '*F*') and the hydrogen-bonded counterparts (denoted '*HB*'), and the subsequent relaxation process from the hydrogen-bonded state into a state at somewhat elevated temperature (denoted '*T*') . Energy transfer from F to HB occurs with rate k_1; the reverse rate is given by k_{-1}. We assume that vibrational relaxation – with rate k_2 occurs from the HB state, rather than from the F state, into the T state.

If we denote the occupation of each of the states as $N_X^{0,1}$, where *X=F, HB* or *T*, and the superscript denotes ground ('*0*') or excited ('*1*') state. Initially the excitation pulse, characterized by the time-dependent intensity *I(t)*, gives rise to population of N_F^1, the time dependent occupation numbers of states N_X read:

$$\frac{\partial N_F^1}{\partial x} = \sigma_{01} I(t)\left[N_F^0 - N_F^1\right] - k_1 N_F^1 + k_{-1} N_{HB}^1$$

$$\frac{\partial N_{HB}^1}{\partial x} = +k_1 N_F^1 - k_{-1} N_{HB}^1 - k_2 N_{HB}^1$$

$$\frac{\partial N_T^0}{\partial x} = k_2 N_{HB}^1$$

The forward and backwards rates k_1 and k_{-1} are linked by the Boltzmann factor that accounts for the energy difference between the two levels:

$$k_1 / k_{-1} = \exp\left[-(2750 - 2580)/k_B T\right])$$

Owing to the fact that the differential signals are detected on the background of the steady state SFG signal, the differential SFG signals for the free and hydrogen-bonded OD groups are simply proportional to N_F^1 and N_{HB}^1, both with a contribution (accounting for the long-time signal offset) from N_T^0. We note that the energy transfer process described here is different from the step-wise vibrational relaxation process that we have described before (see, e.g. Ref. [6]).

References

1 Förster, T. *Z. Naturforsch.* **4**, 821 (1940).

2 Woutersen, S. & Bakker, H. J. Resonant intermolecular transfer of vibrational energy in liquid water. *Nature* **402**, 507-509 (1999).

3 Woutersen, S. in *PhD thesis* (University of Amsterdam, 1999).

4 Piatkowski, L., Eisenthal, K. B. & Bakker, H. J. Ultrafast intermolecular energy transfer in heavy water. *Phys. Chem. Chem. Phys.* **11**, 9033-9038, doi:10.1039/b908975f (2009).

5 Sovago, M. *et al.* Vibrational response of hydrogen-bonded interfacial water is dominated by intramolecular coupling. *Phys. Rev. Lett.* **100**, 173901, doi:10.1103/PhysRevLett.100.173901 (2008).

6 Bonn, M. *et al.* Structural Inhomogeneity of Interfacial Water at Lipid Monolayers Revealed by Surface-Specific Vibrational Pump−Probe Spectroscopy. *J. Am. Chem. Soc.* **132**, 14971-14978 (2010).